

1

## Supplementary Information for

2

3 **Surfactant encapsulating N-doped carbon dots with enhanced optical properties as**

4 **selective sensor for Cr(VI) detection**

5 Qiumeng Chen,<sup>a</sup> Nan Li,<sup>a</sup> Yulu Tian,<sup>a</sup> Qian Liu,<sup>b</sup> Xue Zou,<sup>a</sup> Meikun Fan<sup>a</sup> and Zhengjun Gong<sup>\*a,c</sup>

6 <sup>a</sup> Faculty of Geosciences and Environmental Engineering, Southwest Jiaotong University, Chengdu 611756, China

7 <sup>b</sup> School of Life Science and Engineering, Southwest Jiaotong University, Chengdu 610031, China

8 <sup>c</sup> State-province Joint Engineering Laboratory of Spatial Information Technology of High-Speed Rail Safety, Chengdu

9 611756, China

10

11 \* Corresponding author. E-mail addresses: [gzi@swjtu.edu.cn](mailto:gzi@swjtu.edu.cn) (Z. Gong)

12

13

## 14 **Chemicals**

15 All chemicals are analytical grade and can be used without further purification. Ammonium citrate, urea,  
16 cetyltrimethylammonium bromide (CTAB), cetyltrimethylammonium chloride (CTAC), sodium dodecyl benzene  
17 sulfonate (SDBS), sodium dodecyl sulfate (SDS), polyvinylpyrrolidone (PVP), Tween-80, and potassium dichromate  
18 ( $K_2Cr_2O_7$ ) were purchased from Sigma-Aldrich Trading Ltd. The  $K_2Cr_2O_7$  was used to prepare standard Cr(VI)  
19 solution, and the metal ion solutions were made of their nitrates, sulfates or chlorides. All solutions were prepared  
20 with ultrapure water.

## 21 **Instruments and characterization**

22 Fluorescence measurements were performed on a FLS-1000 steady-state/transient fluorescence  
23 spectrometer (Edinburgh, UK). The transmission electron microscopy (TEM) images were carried out on a JEM-  
24 2100F field emission transmission electron microscope (JEOL, Japan). The UV-vis absorption spectra were  
25 measured by USB-2000 UV-Vis Spectrometer (Ocean Optics, USA). X-ray photoelectron spectroscopy (XPS) was  
26 performed on a Thermo Scientific K-Alpha (Thermo Fisher Scientific, USA). The functional groups of the samples  
27 were characterized by Fourier transform infrared (FT-IR) spectroscopy (Perkin-Lamer, USA).

## 28 **Synthesis of N-CDs**

29 The N-CDs was prepared via a solid-state reaction strategy according to previous literature.<sup>1</sup> Briefly,  
30 ammonium citrate (0.2 g) and urea (0.2 g) were ground uniformly. Subsequently, the mixture was heated to 200 °C  
31 for 1.5 h in an oil bath. After that, the N-CDs was purified with ultrapure water, and collected by centrifugation.  
32 Then, the obtained N-CDs solution was filtered with 0.22 μm filter membrane for further use.

## 33 **Synthesis of N-CDs-CTAC**

34 For synthesis of N-CDs-CTAC, 2 mL of the prepared N-CDs solution was mixed with 4 mL of 20 mg mL<sup>-1</sup> CTAC  
35 solution. Then the mixture solution was ultrasound for 30 min to obtain N-CDs-CTAC, which was stored at 4 °C for  
36 further experiments.

37 In order to obtain the optimal optical properties of N-CDs-CTAC, the preparation conditions were optimized,  
38 including the molar ratio of ammonium citrate to urea (1:4~1:8), reaction time (20~120 min), reaction temperature  
39 (140~220 °C), concentration of CTAC (0~20 mM), and the type of surfactants.

## 40 **Fluorescence detection of Cr(VI)**

41 The fluorescence characteristics of N-CDs-CTAC were studied under different excitation wavelengths, and the  
42 excitation and emission slits were set to 0.6 nm and 0.6 nm, respectively. Under the optimal conditions, 200 μL of  
43 different concentrations of Cr(VI) solution were mixed with 600 μL of N-CDs-CTAC solution, then 700 μL of BR  
44 buffer solution (pH=4) was added to above mixture, and start timing immediately. After reaction for 10 min, the  
45 fluorescence was tested at 405 nm excitation wavelength. All of the experiments were repeated three times.

## 46 **Detection of Cr(VI) in real water samples**

47 The real water samples were collected from a lake at Southwest Jiaotong University and a tap at laboratory  
48 to estimate the viability of the proposed sensor. The environmental waters were first centrifuged for 10 minutes,  
49 then treated with a 0.45 μm filter membrane treatment for further use.

50 Fluorescence method: The detection process was the same as the fluorescence detection of Cr(VI) mentioned  
51 above except that the Cr solution was prepared with actual water.

52 Standard 1,5 dtphenylcarbohydrazide spectrophotometric method: First, the 500 μM Cr(VI) stock solution was  
53 prepared with ultrapure water. Then the different volumes of Cr(VI) stock solution were added into the cuvette  
54 and diluted to 5 ml with ultrapure water. After that, 0.05 mL of 1+1 H<sub>2</sub>SO<sub>4</sub> and 0.05 mL of 1+1 H<sub>3</sub>PO<sub>4</sub> were added

55 into above solution. Finally 0.2 mL of 1,5 dtphenylcarbohydrazide solution was further added for chromogenic  
56 reaction, and the absorbance at 540 nm was measured after reaction for 10 minutes. For assaying Cr(VI) in real  
57 samples, the detection process was the same as the standard 1,5 dtphenylcarbohydrazide spectrophotometric  
58 method except that the Cr solution was prepared with actual water.

### 59 **Quantum yield calculation**

60 The relative quantum yields (QY) of N-CDs and N-CDs-CTAC were determined in reference to fluorophore  
61 fluorescein ( $\eta=1.33$ ,  $QY=95\%$ ) in 0.10 M NaOH solution.<sup>2</sup> The slit width and excitation wavelength ( $\lambda_{ex}=405$  nm)  
62 were kept consistent during QY measurements, and the calculation formula of QY is as follows:

$$QY = QY_{ref} \frac{\eta^2 I A_{ref}}{\eta_{ref}^2 A I_{ref}}$$

63

64 In the formula,  $QY_{ref}$  is the quantum yield of the reference compound,  $\eta$  is refractive index of the solvent,  $I$   
65 represents the integrated fluorescence intensity at  $\lambda_{ex}=405$  nm,  $A$  is absorbance at 405 nm. To minimize the  
66 reabsorption effect, the absorbance value at 405 nm is below 0.05.<sup>3</sup>

68 **Table S1** Fluorescence lifetimes of N-CDs, N-CDs-CTAC, and N-CDs-CTAC in the presence of Cr(VI).

Samples	Average $\tau$ (ns)
N-CDs	5.39
N-CDs-CTAC	10.23
N-CDs-CTAC+ Cr(VI)	7.77

69

70 **Table S2** Comparison of materials preparation conditions and Cr(VI) detection with other reported CD-based  
71 fluorescent sensors.

Materials	Synthesis condition	Quantum yield (%)	Linear range ( $\mu\text{M}$ )	LOD ( $\mu\text{M}$ )	Ref.
<b>N-CQDs</b>	Hydrothermal 220 °C, 6 h	22.14	0-500	2.1	4
<b>CCDa</b>	Hydrothermal 180 °C, 4 h	6.2	5-125	1.17	5
<b>MCDb</b>	Hydrothermal 190 °C, 12 h	/	0-35	4	6
<b>CD</b>	Hydrothermal 250 °C, 4 h	39	10-50	0.73	7
<b>ACDsc</b>	Hydrothermal 200 °C, 5 h	8.47	0.5-100	0.034	8
<b>N, SCDs</b>	Hydrothermal 200 °C, 12 h	18.7	1-40	0.52	9
<b>Pn N-CDs</b>	Hydrothermal 180 °C, 12 h	18.41	0-6	0.185	10
<b>N-CDs-CTAC</b>	Solid-state reaction 200 °C, 1.5 h	44.6	0.5-1000	0.04	This work

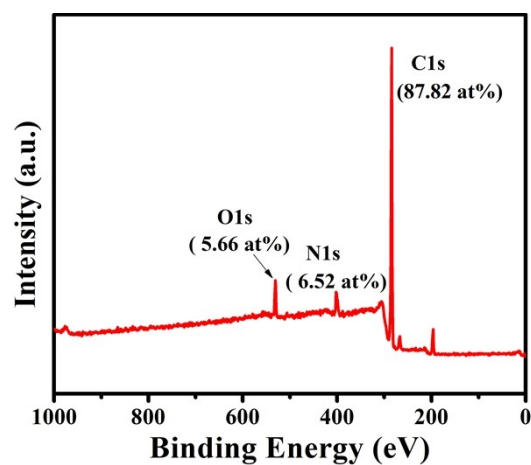
72 a = Cobalt(II)-doped carbon dots

73 b = CD loaded in the porous structure of microcline

74 c = Aqueous soluble CDs

75

76

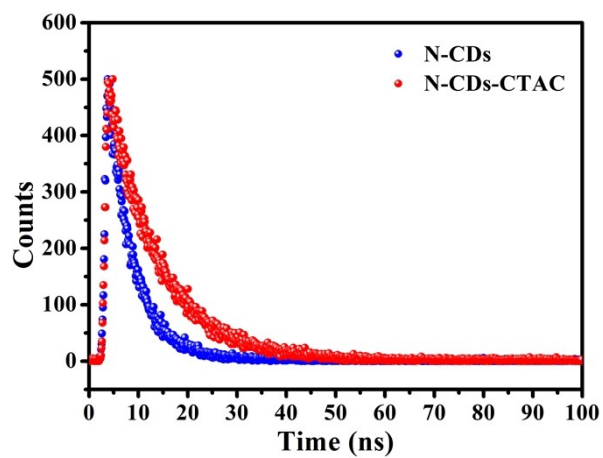


77

78

79

Fig. S1 XPS survey spectrum of N-CDs-CTAC.

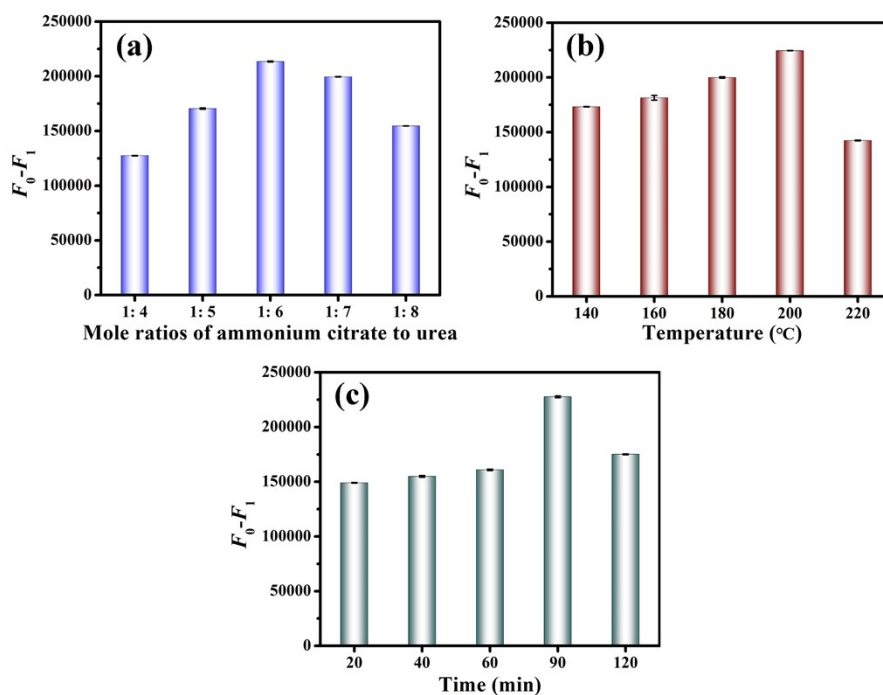


80

81

82

Fig. S2 The fluorescence decay curves of N-CDs and N-CDs-CTAC.

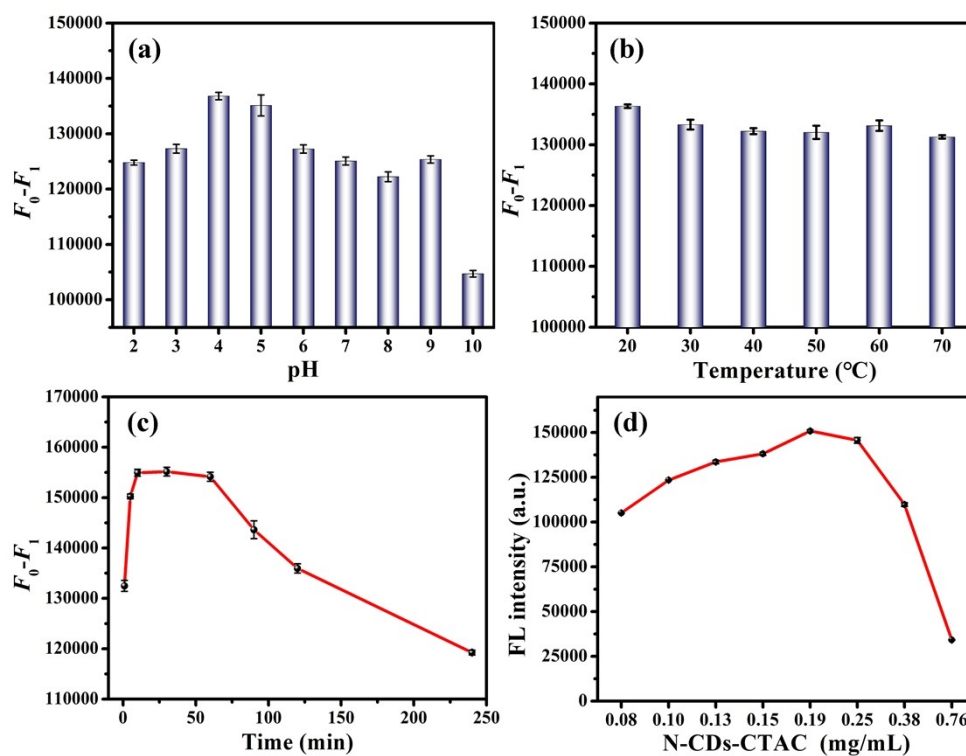


83

84 **Fig. S3** Optimization of preparation conditions for N-CDs. (a) Molar ratio of ammonium citrate to urea, (b) reaction

85 temperature and (c) reaction time.

86

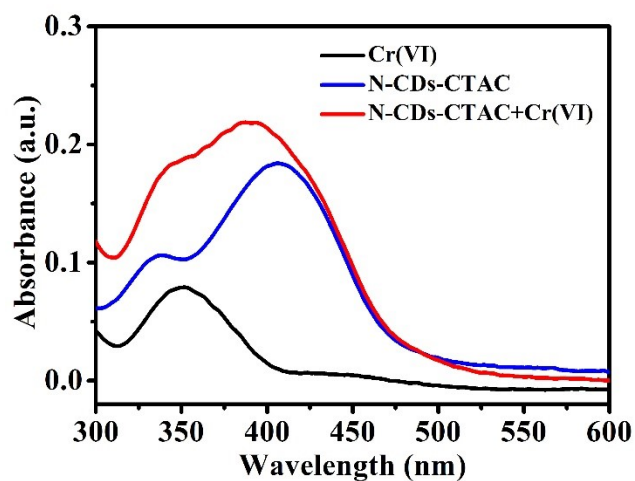


87

88 **Fig. S4** The effects of (a) pH values, (b) incubation temperature, (c) response times, and (d) N-CDs-CTAC

89 concentration on Cr(VI) detection.

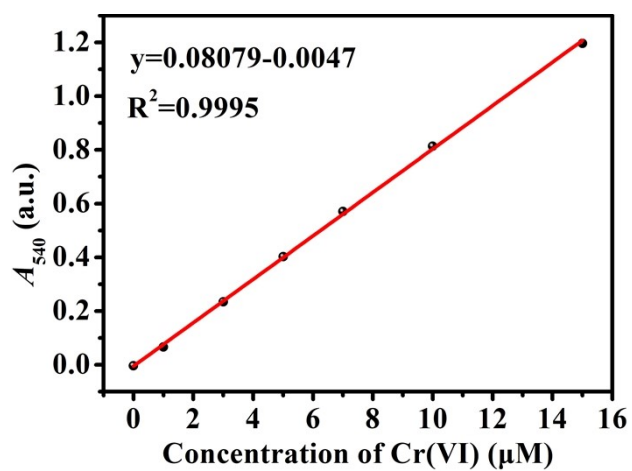
90



91

92 **Fig. S5** The UV-vis absorption spectra of Cr(VI), N-CDs-CTAC, and N-CDs-CTAC with the addition of Cr(VI).

93



94

95 **Fig. S6** The standard curve of Cr(VI) measured by 1,5 dtphenylcarbohydrazide spectrophotometric method.

96

98 **References**

- 99 1 W. U. Khan, D. Wang and Y. H. Wang, *Inorg. Chem.*, 2018, **57**, 15229-15239.
- 100 2 C. Ruiz-Palomero, M. L. Soriano, S. Benítez-Martínez and M. Valcárcel, *Sens. Actuators B Chem.*, 2017, **245**, 946-  
101 953.
- 102 3 M. Zheng, Z. G. Xie, D. Qu, D. Li, P. Du, X. B. Jing and Z. C. Sun, *ACS Appl. Mater. Interfaces*, 2013, **5**, 13242-13247.
- 103 4 G. Q. Wang, S. R. Zhang, J. Z. Cui, W. S. Gao, X. Rong, Y. X. Lu and C. Z. Gao, *Anal. Chim. Acta*, 2022, **1195**, 339478.
- 104 5 H. Y. Zhang, Y. Wang, S. Xiao, H. Wang, J. H. Wang and L. Feng, *Biosens. Bioelectron.*, 2017, **87**, 46-52.
- 105 6 S. Bardhan, S. Roy, D. K. Chanda, S. Ghosh, D. Mondal, S. Das and S. Das, *Dalton Trans.*, 2020, **49**, 10554-10566.
- 106 7 M. R. Pacquiao, M. D. G. de Luna, N. Thongsai, S. Kladsomboon and P. Paoprasert, *Appl. Surf. Sci.*, 2018, **453**, 192-  
107 203.
- 108 8 J. F. Li, P. X. Li, D. X. Wang and C. Dong, *Talanta*, 2019, **202**, 375-383.
- 109 9 J. Shen, S. M. Shang, X. Y. Chen, D. Wang, Y. Cai, *Sensor. Actuator. B Chem.*, 2017, **248**, 92e100.
- 110 10 X. D. Zheng, K. H. Qin, L. P. He, Y. F. Ding, Q. Luo, C. T. Zhang, X. M. Cui, Y. Tan, L. N. Li and Y. L. Wei, *Analyst*,  
111 2021, **146**, 911-919.
- 112